A Fast Two Dimensional FDTD Full-Wave Analyser with Adaptive Mesh Size

W-3

S. Xiao, R. Vahldieck and H. Jin

Laboratory for Lightwave Electronics, Microwave and Communications
(LLiMiC)
Department of Electrical and Computer Engineering
University of Victoria
Victoria, B.C., Canada, V8W 3P6

Abstract

A two-dimensional variable Yee's mesh algorithm with reduced grid size is proposed for the full-wave analysis of arbitrarily shaped guided wave structures. The method includes losses and allows the frequency selective application of the FDTD method. The continuously variable mesh size in x- and y-direction makes it possible to resolve partially fine circuit structures in both dimensions, while in other circuit sections a coarse mesh size can still be used.

Introduction

The TDFD has been well established as a versatile full-wave technique to solve electromagnetic field problems [1-13]. Although the method has many attractive features for time domain problems, a very fine mesh size must be used in order to resolve the non-uniform fields in MICs or MMIC's. Fine mesh sizes on the other hand, lead to excessive computer memory and run-time, which renders this method not very effective in the frequency selective design of microwave circuits.

In order to alleviate the extensive CPU-time requirements of the TDFD (at least on workstations and serial machines), different forms of graded meshes were used in the past with variable success. The basic problem in utilizing any grading scheme is that the larger the mesh ratio, the higher the time-domain errors which lead to significant errors in the frequency domain, since the Fourier transform is very sensitive to errors in the time domain impulse.

Two different ways of grading a TDFD mesh were proposed so far. Hoefer et.al. [10] introduced a grading scheme in which the mesh size in y-direction was different from that in x-direction but the mesh size were kept constant in either direction (Fig.1b). Zivanovic et.al. [13] recently published a subgridding method in which sections of the overall mesh contained a fine mesh size. The mesh size within as well as outside this section were also kept constant (Fig.1c). The common feature of both grading schemes is that the mesh size is regionally constant.

In this paper we are analyzing a third grading scheme which is gradually changing its mesh size in either x- or y-direction or in both directions simultaneously (Fig.1d). This grading scheme is generally rejected by other researchers in this field because the time domain error introduced is of first order and it was not possible so far to reduce this error to second order. In spite of this fact, the variable mesh scheme has been utilized in [9]. Without improving the algorithm, the authors of [9] stated that the variable grading scheme can be used without significant errors. This statement is not justified, because the error in this method is still of first order and the results reported in that paper were found by using a very small mesh ratio. So it is not surprising that the results obtained with a variable mesh size are close to the ones obtained with a uniform mesh size.

The scheme presented in this paper utilizes the variable grading mesh shown in Fig.1d, but improves the accuracy from first order to second order by analytical cancellation of the first order error term. Furthermore, this paper also introduces a scheme to use the time domain solution procedure of the FDTD for frequency selective applications of this method.

An adaptive mesh algorithm with second order accuracy

In order to demonstrate this new idea and to keep the problem simple, we first of all assume a uniform mesh along the z-direction without loss of generality. The z-direction can be easily implemented into this scheme. In each mesh cell the magnetic field components can always be arranged in the centre (central finite difference) and a second order accuracy can be maintained throughout when calculating H-components from the E-components. However, in the variable grading mesh the E-field (E2 in Fig.2) is not located in the middle between H1 and H2 and therefore calculating the E-field from the H-field leads to a first order error. This is illustrated by looking into the expression for the Ex-field as an example:

$$E_x^{n+1}(i,j,k) = E_x^n(i,j,k) + \frac{\Delta t}{\varepsilon_x}\left[\frac{\partial H_z^{n+0.5}(i,j,k)}{\partial x} - \frac{\partial H_y^{n+0.5}(i,j,k)}{\partial z}\right] \tag{1a}$$

Developing the x-dependent term in this equation by a Taylor series yields:

$$\frac{\partial H_z^{n+0.5}(i,j,k)}{\partial x} = \frac{H_z^{n+0.5}(i,j+1,k) - H_z^{n+0.5}(i,j,k)}{\Delta h(q_j + q_{j+1})/2} + o((q_{j+1} - q_j)\Delta h) \tag{1b}$$

which clearly shows that normally a variable grading scheme provides only first order accuracy.

However, by including the three neighbouring mesh cells, it is possible to eliminate the first order error term, and a second order accuracy is obtained.

$$\frac{\partial H_z^{n+0.5}(i,j,k)}{\partial x} = \frac{H_z^{n+0.5}(i,j+1,k) - H_z^{n+0.5}(i,j,k)}{\Delta h(q_j + q_{j+1})/2}$$

CH3141-9/92/0000-0783$01.00 © 1992 IEEE

$$+d_j\left[\frac{H_z^{n+0.5}(i,j+2,k)-H_z^{n+0.5}(i,j+1,k)}{\Delta h(q_{j+1}+q_{j+2})/2}-\right.$$

$$\left.\frac{H_z^{n+0.5}(i,j,k)-H_z^{n+0.5}(i,j-1,k)}{\Delta h(q_{j-1}+q_j)/2}\right]+o(\Delta h^2) \tag{1c}$$

d_j (j=1, 2,...,N) is time independent and fixed for a specific mesh arrangement. The first and second terms in the bracket of the above equation have been calculated in the neighbouring equations and therefore, the new algorithm requires no more computations than the algorithm in (1a).

Frequency selective FDTD with adaptive mesh size

The application of the FDTD for frequency selective circuit analysis and design requires significant computer resources. This is so because processing a time domain impulse involves from the start the entire frequency spectrum. Only after the processing, the frequency spectrum of interest is selected. This requires not only significant CPU-time, but also memory since, up to now, any full-wave analysis with the FDTD requires a three-dimensional mesh. Although this is generally a disadvantage of the FDTD, the flexibility of the method in terms of its suitability to analyze arbitrary geometry sometimes outweights the demand for significant computer resources.

In this part of the paper we introduce a frequency selective FDTD algorithm with only a half-size two-dimensional mesh. This technique preserves the advantageous features of the conventional FDTD, but it can only be used in the frequency domain, and is therefore very attractive for CAD of MIC's and MMIC's.

This new technique uses only a two-dimensional mesh consisting of a three-dimensional space grid for the analysis of hybrid modes. This two-dimensional mesh could also be regarded as one slice out of a three-dimensional mesh, with the third dimension, the propagation direction, being replaced by introducing a phase shift. This step allows also to reduce the size of the space grid to only half of it's normal size. At a first glance, introducing a phase shift in the time domain algorithm seems to be an odd approach. However, by choosing the propagation constant and then exciting the system with a time domain impulse provides correct results (after a Fourier transform) only at the frequency at which this propagation constant is valid. This step must then be repeated for different propagation constants to obtain the dispersion curve for that particular mode. Since this approach requires only a two-dimensional mesh with a half-size space grid and since the propagation constant is given as an input parameter, the algorithm convergences much faster than in the conventional approach and the memory space is reduced significantly. Moreover, this approach can handle losses easily. To improve the algorithm even further, we have included the technique for the variable mesh size as described before.

The new approach follows the two-step leap-frog FDTD procedure initially developed for a full sized three-dimensional grid. When the field components are normalized by the free-space impedance $Z_0 = \sqrt{\mu_0 / \varepsilon_0}$ $Z_0 = \sqrt{\mu_0 / \varepsilon_0}$

$$E_{x,y,z}^n(i,j,k) = e_{x,y,z}^n(i,j,k)\sqrt{Z_0}$$
$$H_{x,y,z}^{n+0.5}(i,j,k) = h_{x,y,z}^{n+0.5}(i,j,k)/\sqrt{Z_0} \tag{2}$$

Considering the arbitrary variable mesh as shown in Fig.1f, the magnetic fields are arranged in the middle of the mesh to have a second order accuracy when calculating the magnetic fields via the electric fields. The mesh parameters p_i (i=1,2,...,M), q_j (j=1,2,...,N), and r_k (k=1,2,...,K) are any positive real number as required to resolve the specific structure. s=c $\Delta t/\Delta h$, Δt and Δh are, respectively, the time and the space steps. The mesh dimension is shown in Fig.1. If p_i=constant (i=1,2,...,M), q_j=constant (j=1,2,...,N) and r_k =constant (k=1,2,...,K), the new mesh will be reduced to the same rectangular one as in [10]. If all mesh parameters along the x-, y-, and z-direction are set to unity, the mesh size will be uniform.

After the mesh size has been made variable, a phase shift $r_k\beta\Delta h$ is now introduced at any adjacent nodes for any specific propagation constant β. This modal knowledge is now used to simplify the scheme. It is easy to see that any incident or reflected impulse for any propagation constant β satisfies [15]:

$$e_p^n(i,j,k\pm1) = e_p^n(i,j,k)\exp\{\mp j\beta r_k\Delta h\}$$
$$h_p^n(i,j,k\pm1) = h_p^n(i,j,k)\exp\{\mp j\beta r_k\Delta h\} \quad , \quad p = x,\ y,\ z \tag{3}$$

Because the mesh in z-direction is closed in itself, the mesh parameters are set to unity along this axis. The new variable mesh algorithm can be written as

$$h_x^{n+0.5}(i,j) = h_x^{n-0.5}(i,j) - s\left\{\left(e_z^n(i,j+1) - e_z^n(i,j)\right)/q_j + 2\sin(\beta\Delta h/2)e^{j(\pi-\beta\Delta h)/2}e_j^n(i,j)\right\}/\mu_{rx}$$

$$e_x^{n+1}(i,j) = e_x^n(i,j) + 2s\{(h_z^{n+0.5}(i,j) - h_z^{n+0.5}(i,j-1))/(q_j + q_{j-1}) + l_i - 2\sin(\beta\Delta h/2)e^{-j(\pi-\beta\Delta h)/2}\, h_y^{n+0.5}(i,j)\}/\varepsilon_{rx} \tag{4}$$

Similarly for the other field components. From equ. (4) it is obvious that now only a two-dimensional mesh is involved. l_i is the compensation factor related to the neighboring mesh sizes similar to (1c). Since this process closes the z-direction in itself, only a reduced space grid of half size remains (Fig.1f) and no absorbing-wall or shorted-shielding is needed along the propagation direction.The grid size in z-direction is arbitrary as long as the transmission line is homogeneous in this direction.

The losses can be easily taken into consideration by using the complex relative dielectric constant in the scheme. This self-consistent approach applied in the new TDFD mesh holds for any kind of losses and also for metallization dimensions smaller, comparable or larger than the skin depth [16]. The

attenuation factor can be calculated from the Fourier transformation of the impulse at a specific space point and at different time steps after mode stability has been reached.

Numerical Results

To verify the accuracy of this new frequency selective TDFD approach, we have first compared analytical results for the air- and dielectric-filled rectangular waveguide with our numerical calculations. The excellent agreement is demonstrated in Fig.2. Here only the dominant mode is chosen as excitation. For the Fourier transformation, the Blackman window has been utilized because of its smooth shape [14].

To illustrate the advantages of the two-dimensional variable mesh versus the uniform mesh, Fig.3 shows a comparison for the calculation of the microstrip propagation constant. The variable mesh used is shown in Fig.1e. The horizontal axis in Fig.3 denotes the mesh ratio, which equals one for the limiting case of the uniform mesh. It is clearly seen that up to a ratio of 4:1, the CPU time is only 5% of that of the uniform mesh and the error is less than 1%.

To demonstrate the capability of this new approach we have calculated the CPW and the microstrip conductor losses (including ground plane losses) considering finite metallization thickness and dielectric losses. The results are shown in Fig.4 and Fig.5 for very small conductor dimensions.

Conclusion

A 2-D TDFD variable or adaptive mesh with second order accuracy for the full-wave analysis of inhomogeneous transmission lines has been introduced. Together with only a half-size space grid the memory space and CPU-time of the TDFD has been reduced significantly. Introducing a phase shift in axial direction and chosing the propagation constant as input parameter, allows a frequency selective application of the TDFD. This makes the TDFD a very efficient tool for practical CAD of various complicated microwave circuits.

Reference

[1] T.Shibata,T.Hayashi and T.Kimura,"Analysis of microstrip circuits using three dimensional full-wave electromagnetic field analysis in the time domain", IEEE Trans. Microwave Theory Tech., pp.1064-1070,vol.MTT-36,no.6,1988

[2] K.S. Yee, "Numerical solution of initial boundary value problems involving Maxwell's equations in isotropic media", IEEE Trans. Antennas Propagat., vol.AP-14, pp.302-307, May 1966.

[3] X. Zhang, J. Fang, K.K. Mei and Y. Liu, "Calculations of the dispersive characteristics of microstrips by the time-domain finite difference method", IEEE Trans. Microwave Theory Tech., vol.MTT-36, pp.263-267, Feb. 1988.

[4] D.H. Choi and W.J.R. Hoefer, "The finite difference time domain method and its application to eigenvalue problems", IEEE Trans. Microwave Theory Tech., vol.MTT-34, pp.1464-1470, 1986.

[5] M. Rittweger and I. Wolff, "Analysis of complex passive (M)MIC-components using the finite difference time-domain approach", pp.1147-1150, 1990 IEEE MTT-S digest.

[6] X. Zhang and K.K. Mei, "Time-domain finite difference approach to the calculation of the frequency-dependent characteristics of microstrip discontinuities", IEEE Trans. Microwave Theory Tech., vol.MTT-36, pp.1775-1787, 1988.

[7] W.K.Gwarek,"Microwave circuits designed by two-dimensional vector wave equation and their analysis by FDTD method", pp.866-871, 21th European Microwave Conf. Digest, German,Sept., 1991.

[8] W.K.Gwarek,"Analysis of an arbitrarily-shaped planar circuit-a time domain approach", IEEE Trans. Microwave Theory Tech., vol.MTT-33,no.10, pp.1067-1072, 1985

[9] D.L.Paul, E.M.Daniel, C.J.Railton, "Fast finite difference time domain method for the analysis of planar microstrip circuits", pp.303-308, 21th European Microwave Conference, German, Sept., 1991.

[10] D.H.Choi and W.F.R.Hoefer, "A graded mesh FDTD algorithm for eigenvalue problems", pp.413-417, 17th European microwave conference, 1987.

[11] X.Zhang and K.K.Mei, "Time domain calculation of microstrip components and curve-fitting of numerical results", pp.313-316, 1989 MTT-S Digest.

[12] X.Zhang,"Time domain finite difference analysis of the frequency-dependent characteristic of the microstrip discontinuities", Master Thesis, Dept. of EECS, Univ. of California, Berkeley, Nov., 1987.

[13] S.S.Zivanovic, K.S.Yee, K.K.Mei,"A subgridding method for the time-domain finite-difference method to solve Maxwell's equations",pp.471-479,

[14] A.V. Oppenheim and R.W. Schafer, *"Digital Signal Processing"*, Prentice-Hall, Inc., 1975

[15] H. Jin, R. Vahldieck and S. Xiao, "An improved TLM full-wave analysis using two dimensional mesh", pp.675-677, 1991 IEEE-S International Microwave Symposium Digest, Boston, MA, Jun. 1991.

[16] W.Heinrich,"Full-wave analysis of conductor losses on MMIC transmission lines",pp.911-915,1989 MTT-S Digest.

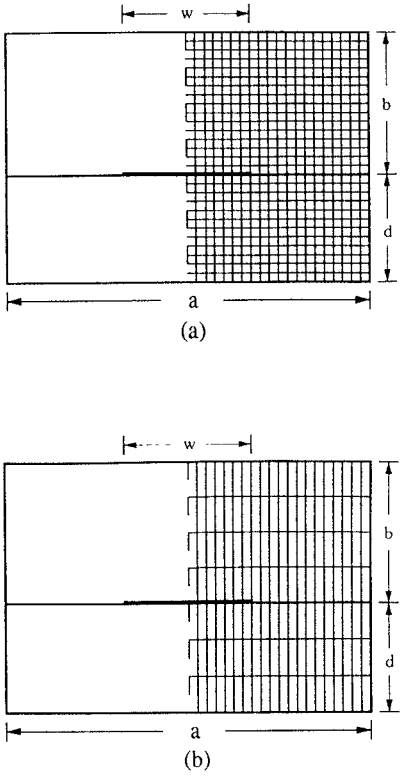

Fig.1

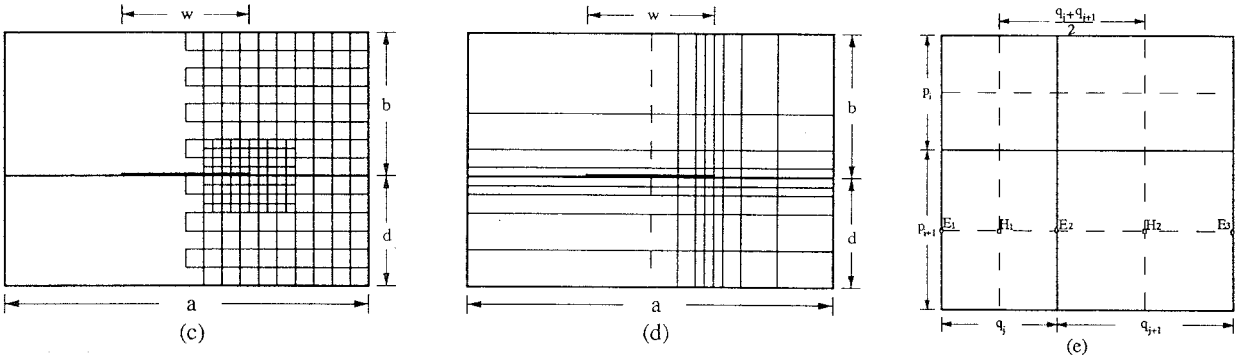

Fig.1 FDTD meshes (a)Uniform; (b)Rectangular; (c)Subgridding; (d)Adaptive variable; (e)A zoomed section of neighbouring meshes from (d); (f)A variable mesh with half size of Yee's

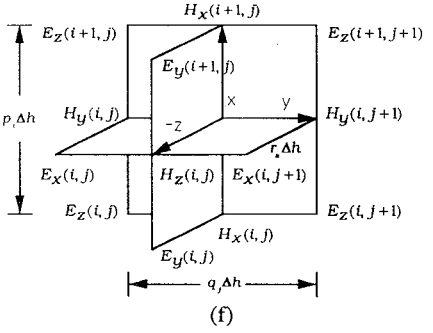

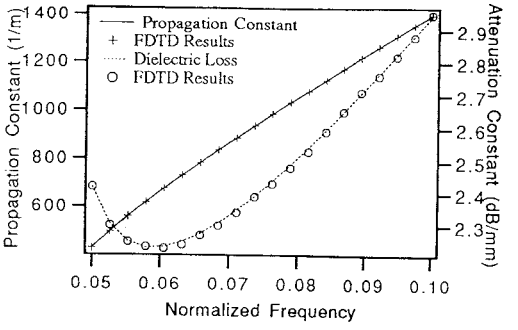

Fig.2 Comparison between FDTD results and analytical solution for a dielectric-filled rectangular waveguide (a=2b=7.11mm, tg $\delta = 4.10^{-4}$, e_r=12.8)

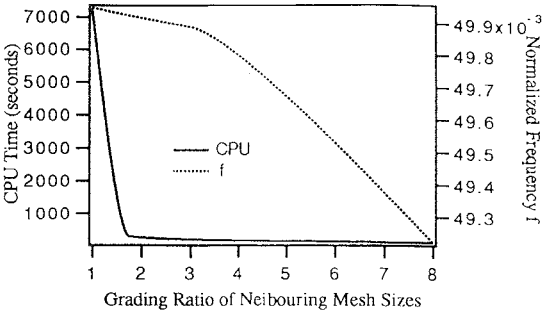

Fig.3 CPU time and accuracy comparison between different mesh size ratios for a microstrip line in Fig.1d (d/λ =1, a/d=7, b/d=3, ε_r=9.0, w/d=2)

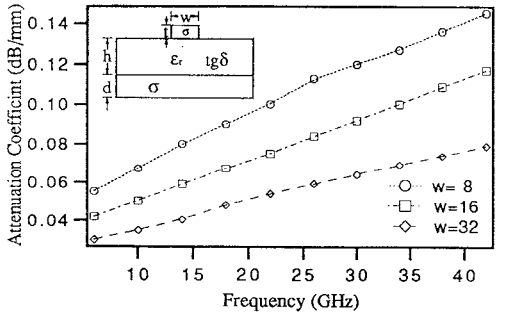

Fig.4 Frequency dependency of attenuation coefficient for a GaAs microstrip line, h=100 μm, ε_r=12.8, tg $\delta = 4.10^{-4}$, σ=4.1 10^7 s/m, t=4 μm, d=8 μm.

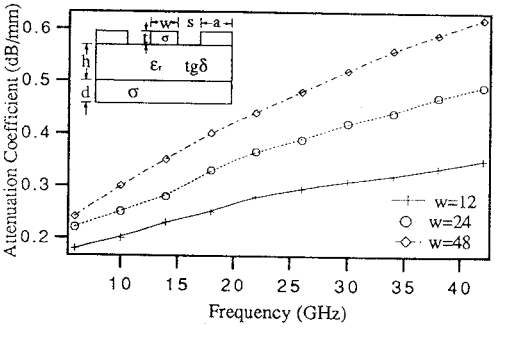

Fig.5 Frequency dependency of attenuation coefficient for a GaAs CPW line, h=200 μm, ε_r=12.8, tg $\delta = 4.10^{-4}$, σ=4.1 10^7 s/m, t=4 μm, d=8 μm, s=8 μm, a=50 μm.